

# Vapor–Liquid Equilibrium Data of the Carbon Dioxide + Ethyl Butyrate and Carbon Dioxide + Propylene Carbonate Systems at Pressures from (1.00 to 13.00) MPa and Temperatures from (313.0 to 373.0) K

Li Hongling,<sup>†,‡</sup> Zhu Rongjiao,<sup>\*,†</sup> Xu Wei,<sup>§</sup> Li Yanfen,<sup>†</sup> Su Yongju,<sup>†</sup> and Tian Yiling<sup>†</sup>

<sup>†</sup>Department of Chemistry, School of Science, Tianjin University, Tianjin, 300072 China

<sup>‡</sup>School of Chemistry and Chemical Engineering, Shihezi University, Shihezi, 832003 China

<sup>§</sup>SINOPEC Safety Engineering Institute, Qingdao, 266071 China

**ABSTRACT:** High-pressure vapor–liquid equilibrium data for the binary systems of ethyl butyrate (EB) + carbon dioxide and propylene carbonate (PC) + carbon dioxide were measured. The experimental pressure range was from (1.00 to 13.00) MPa and the temperature range from (313.0 to 373.0) K. Experimental results were correlated with the Peng–Robinson equation of state with the two-parameter van der Waals mixing rule. At the same time, the Henry's coefficient and solution enthalpy and solution entropy of CO<sub>2</sub> during dissolution at different temperature were also calculated.

## INTRODUCTION

Vapor–liquid equilibrium (VLE) data containing supercritical (SC) CO<sub>2</sub> are important for the design, development, and operation of supercritical fluid separation processes. The main method of obtaining phase equilibrium data is by experimentation. Several review articles on high-pressure fluid phase equilibrium experimental methods and investigated systems have been published.<sup>1–3</sup> Most of these studies have focused on supercritical carbon dioxide because it is an inexpensive, nontoxic, and environmentally benign solvent. In separation process it leaves no solvent residues in products. The high diffusivity, low viscosity, and low surface tension of SC CO<sub>2</sub> are expected to speed up mass-transfer controlling chemical reactions or extractions. From the mid-1980s, the SC CO<sub>2</sub> + alcohol, esters, and ethers systems are of interest because of their importance as SC CO<sub>2</sub>/cosolvent pairs in the biomaterials and pharmaceutical industry.<sup>4–6</sup> We have constructed an autoclave consisting of a cylindrical steel cell to investigate high-pressure phase equilibria.<sup>7,8</sup>

In this study, we measured the VLE data for two binary mixtures of SC-carbon dioxide with ethyl butyrate (EB) and propylene carbonate (PC). Ethyl butyrate is used as perfume or aroma additives for cosmetics and food industries. Propylene carbonate is used as the electrolyte component for lithium batteries, polar solvents and chemical intermediates. In the previous work, the VLE data of SC carbon dioxide + propylene carbonate and propylene carbonate systems have been reported,<sup>9–13</sup> but the density  $\rho$  and mole volume  $V_m$  were not provided or in narrow  $P$ – $T$  ranges. This paper presents the new data of  $p$ ,  $T$ ,  $x$ ,  $y$ ,  $\rho$ , and  $V_m$  for the two binary systems at (313.0, 333.0, 353.0, and 373.0) K, with pressure range from (1.00 to 13.00) MPa.

## EXPERIMENT SECTION

**Materials and Their Purities.** Carbon dioxide (molar fraction purity >0.9999) was provided by Tianjin Special Gas limited Company, and the ethyl butyrate and propylene carbonate (mass

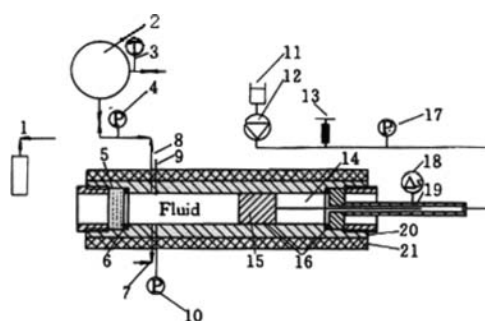


**Figure 1.** Schematic diagram of the high-pressure apparatus: 1, small steel vessel; 2, glass bulb; 3, thermometer; 4, pressure sensor; 5, window; 6, O-ring; 7, valve; 8, capillary; 9, thermocouple; 10, pressure sensor; 11, oil reservoir; 12, pump; 13, screw-driven pump; 14, oil; 15, piston; 16, O-ring; 17, pressure meter; 18, Hall probe; 19, magnet; 20, autoclave; 21, heat jacket.

**Table 1.** Critical Data ( $p_{c,i}$ ,  $T_{c,i}$ ) and Acentric Factors ( $\omega$ 's) of the Pure Components

substance	$T_c$ /K	$p_c$ /MPa	$\omega$
carbon dioxide	304.2	7.37	0.225
ethyl butyrate	569.0	2.96	0.461
propylene carbonate	625.2	5.71	0.707

fraction purity >0.9985) were supplied by Aladdin Reagent Company. They were degassed before used at 268.0 K for 2 h.

**Special Issue:** John M. Prausnitz Festschrift

**Received:** October 24, 2010

**Accepted:** March 1, 2011

**Published:** March 21, 2011

Table 2. Vapor–Liquid Equilibrium Data of CO<sub>2</sub> (1) + EB (2) and CO<sub>2</sub> (1) + PC (2) Systems at Various Temperatures and Pressures

<i>p</i> /MPa	<i>x</i> <sub>1</sub>	$\rho_L/g \cdot cm^{-3}$	$V_{m,L}/cm^3 \cdot mol^{-1}$	CO <sub>2</sub> (1) + EB (2)		$\rho_V/g \cdot cm^{-3}$	$V_{m,V}/cm^3 \cdot mol^{-1}$	<i>K</i> <sub>1</sub>	<i>K</i> <sub>2</sub>
				<i>y</i> <sub>1</sub>					
<i>T</i> /K = 313.0									
2.00	0.3795	0.9191	96.59	0.9978	0.0394	1120.78	2.629	0.0035	
3.00	0.4919	0.9010	89.53	0.9926	0.0613	726.73	2.018	0.0146	
4.00	0.6053	0.8676	83.54	0.9951	0.0968	458.20	1.644	0.0124	
5.00	0.7204	0.8413	76.28	0.9938	0.1412	314.78	1.380	0.0222	
6.00	0.8124	0.8138	70.70	0.9941	0.2229	199.31	1.224	0.0314	
7.00	0.8876	0.7898	65.98	0.9888	0.3000	149.36	1.114	0.0996	
8.00	0.9495	0.7448	63.97	0.9616	0.4500	103.94	1.013	0.7604	
<i>T</i> /K = 333.0									
2.00	0.3088	0.8015	117.13	0.9670	0.0382	1214.17	3.131	0.0477	
3.00	0.3978	0.8069	108.39	0.9751	0.0570	803.45	2.451	0.0413	
4.00	0.4910	0.8044	100.37	0.9726	0.0824	558.04	1.981	0.0538	
5.00	0.5707	0.7868	95.30	0.9713	0.1205	382.33	1.702	0.0669	
6.00	0.6514	0.7813	88.51	0.9709	0.1642	280.75	1.490	0.0835	
7.00	0.7285	0.7522	84.54	0.9706	0.2581	178.67	1.332	0.1083	
8.00	0.8105	0.7266	79.37	0.9716	0.2984	154.34	1.199	0.1499	
9.00	0.8711	0.6920	77.02	0.9541	0.3751	126.14	1.095	0.3561	
10.00	0.9039	0.6700	76.03	0.9200	0.4265	116.70	1.018	0.8325	
<i>T</i> /K = 353.0									
2.00	0.2195	0.7629	131.50	0.9121	0.0345	1458.41	4.155	0.1126	
3.00	0.2919	0.7647	124.37	0.9126	0.0462	1088.42	3.126	0.1234	
4.00	0.3560	0.7658	118.14	0.9151	0.0685	732.31	2.571	0.1318	
5.00	0.4259	0.7588	112.58	0.9166	0.1065	469.72	2.152	0.1452	
6.00	0.4863	0.7530	107.67	0.9166	0.1504	332.64	1.885	0.1623	
7.00	0.5364	0.7348	105.41	0.9189	0.2159	230.93	1.713	0.1750	
8.00	0.5983	0.7196	101.43	0.9142	0.2580	194.54	1.528	0.2136	
9.00	0.6685	0.6851	99.15	0.9127	0.3083	163.13	1.365	0.2632	
10.00	0.7399	0.6558	95.71	0.9100	0.3317	152.22	1.230	0.3461	
11.00	0.8222	0.6552	86.73	0.8900	0.3750	138.50	1.082	0.6187	
<i>T</i> /K = 373.0									
2.00	0.1800	0.6273	164.46	0.8670	0.0306	1752.02	4.817	0.1621	
3.00	0.2406	0.6654	148.47	0.8751	0.0451	1174.67	3.637	0.1645	
4.00	0.3086	0.6755	139.01	0.8726	0.0647	822.28	2.828	0.1843	
5.00	0.3859	0.6865	128.64	0.8713	0.0965	552.31	2.258	0.2096	
6.00	0.4129	0.6750	127.95	0.8709	0.1264	421.90	2.109	0.2199	
7.00	0.4862	0.6594	122.95	0.8706	0.1710	311.92	1.790	0.2519	
8.00	0.5222	0.6474	121.22	0.8716	0.2011	264.88	1.669	0.2687	
9.00	0.5764	0.6399	116.54	0.8766	0.2332	226.88	1.521	0.2913	
10.00	0.6256	0.6288	112.93	0.8560	0.2598	209.39	1.368	0.3846	
11.00	0.6579	0.6163	111.45	0.8521	0.2899	188.62	1.295	0.4323	
12.00	0.6875	0.5832	114.11	0.8153	0.3129	183.21	1.186	0.5911	
<i>p</i> /MPa	<i>x</i> <sub>1</sub>	$\rho_L/g \cdot cm^{-3}$	$V_{m,L}/cm^3 \cdot mol^{-1}$	CO <sub>2</sub> (1) + PC (2)		$\rho_V/g \cdot cm^{-3}$	$V_{m,V}/cm^3 \cdot mol^{-1}$	<i>K</i> <sub>1</sub>	<i>K</i> <sub>2</sub>
				<i>y</i> <sub>1</sub>					
<i>T</i> /K = 313.0									
2.00	0.2593	1.1700	74.38	0.9953	0.0476	930.50	3.838	0.0063	
3.00	0.3384	1.1700	70.45	0.9895	0.0730	611.51	2.924	0.0159	
4.00	0.4022	1.1600	67.87	0.9864	0.0972	460.83	2.452	0.0228	
5.00	0.4548	1.1648	64.96	0.9894	0.1368	326.14	2.175	0.0195	
6.00	0.4919	1.1560	63.59	0.9963	0.1705	259.33	2.026	0.0073	

Table 2. Continued

$p/\text{MPa}$	$x_1$	$\rho_L/\text{g}\cdot\text{cm}^{-3}$	$\text{CO}_2$ (1) + PC (2)		$\rho_V/\text{g}\cdot\text{cm}^{-3}$	$V_{m,V}/\text{cm}^3\cdot\text{mol}^{-1}$	$K_1$	$K_2$
			$V_{m,L}/\text{cm}^3\cdot\text{mol}^{-1}$	$y_1$				
7.00	0.5420	1.1414	61.86	0.9900	0.2247	198.44	1.827	0.0218
8.00	0.5706	1.1297	61.03	0.9900	0.2440	182.74	1.735	0.0233
9.00	0.6169	1.1092	59.73	0.9907	0.2767	160.96	1.606	0.0243
10.00	0.6579	1.0893	58.64	0.9841	0.3399	132.16	1.496	0.0465
11.00	0.6915	1.0730	57.71	0.9866	0.3662	122.27	1.427	0.0435
12.00	0.7279	1.0466	57.14	0.9694	0.3908	117.14	1.332	0.1125
$T/\text{K} = 333.0$								
3.00	0.2425	1.0907	80.69	0.9942	0.0520	852.63	4.100	0.0077
4.00	0.2787	1.0967	78.33	0.9968	0.0778	567.94	3.577	0.0044
5.00	0.3272	1.1067	75.07	0.9922	0.1002	443.64	3.032	0.0116
6.00	0.3723	1.1057	72.77	0.9862	0.1168	383.44	2.649	0.0220
7.00	0.4079	1.1092	70.68	0.9885	0.1479	301.95	2.423	0.0194
8.00	0.4512	1.1102	68.35	0.9898	0.1745	255.53	2.194	0.0186
9.00	0.4846	1.1022	67.08	0.9840	0.1996	225.12	2.030	0.0310
10.00	0.5244	1.0912	65.64	0.9855	0.2302	194.82	1.879	0.0305
11.00	0.5725	1.0771	63.90	0.9812	0.2713	166.22	1.714	0.0441
12.00	0.6065	1.0611	63.01	0.9888	0.3265	136.78	1.630	0.0285
13.00	0.6246	1.0525	62.52	0.9883	0.4112	108.66	1.582	0.0312
$T/\text{K} = 353.0$								
1.00	0.0810	1.0110	96.33	0.9520	0.0186	2515.50	11.755	0.0522
2.00	0.1150	1.0245	93.13	0.9663	0.0322	1427.26	8.404	0.0381
3.00	0.1518	1.0300	90.56	0.9679	0.0509	901.07	6.376	0.0378
4.00	0.1960	1.0408	87.15	0.9679	0.0685	669.56	4.939	0.0399
5.00	0.2317	1.0443	84.87	0.9591	0.0844	549.48	4.139	0.0532
6.00	0.2852	1.0548	81.08	0.9866	0.1000	447.78	3.459	0.0187
7.00	0.3205	1.0624	78.57	0.9836	0.1150	390.89	3.069	0.0241
8.00	0.3510	1.0500	77.81	0.9922	0.1645	270.23	2.827	0.0120
9.00	0.3881	1.0484	75.88	0.9891	0.2060	216.67	2.549	0.0178
10.00	0.4112	1.0355	75.52	0.9709	0.2247	203.34	2.361	0.0494
11.00	0.4485	0.9975	76.23	0.9779	0.2500	181.14	2.181	0.0401
12.00	0.4920	0.9704	75.75	0.9719	0.3000	152.11	1.975	0.0553
13.00	0.5225	0.9511	75.43	0.9842	0.3200	140.37	1.884	0.0331
$T/\text{K} = 373.0$								
3.00	0.1384	1.0000	94.05	0.9747	0.0400	1136.74	7.043	0.0294
4.00	0.1638	1.0049	92.12	0.9779	0.0605	748.49	5.970	0.0264
5.00	0.2031	1.0054	89.80	0.9800	0.0827	546.09	4.825	0.0251
6.00	0.2367	1.0115	87.34	0.9802	0.0959	470.80	4.141	0.0259
7.00	0.2692	1.0000	86.45	0.9784	0.1259	359.45	3.634	0.0296
8.00	0.2948	0.9889	85.92	0.9795	0.1498	301.67	3.323	0.0291
9.00	0.3268	0.9809	84.73	0.9782	0.1580	286.50	2.993	0.0324
10.00	0.3403	0.9608	85.68	0.9847	0.1810	248.00	2.894	0.0232
11.00	0.3805	0.9407	85.03	0.9806	0.2268	198.97	2.577	0.0313
12.00	0.3900	0.9351	84.95	0.9848	0.2417	185.70	2.525	0.0249
13.00	0.4136	0.9312	83.83	0.9844	0.2649	169.52	2.380	0.0266

**Experimental Apparatus and Procedures.** The experimental apparatus used is shown in Figure 1.<sup>7,8</sup> The main part of the apparatus is a high-pressure view cell of 100 cm<sup>3</sup>. There is a moveable piston inside the cylinder autoclave. The piston separates the content in the cell from the pressure medium. The pressure was generated with a manually operated screw-driven pump and was measured with a pressure sensor. This

pressure sensor (model CYB-20S) with a certainty of  $\pm 0.05\%$  and the pressure displayer (model DP-A) were previously calibrated by a standard pressure gauge. The quartz window allowed to observe the phase behavior of the content inside the autoclave. For better mixing, the content inside the autoclave was stirred with a magnetic stirrer. The temperature was measured with a calibrated chromel-alumel thermocouple

inside the cell. The accuracy of the pressure was  $\pm 0.01$  MPa, and the accuracy of the temperature was  $\pm 0.1$  K.

Before each measurement, the view cell was first evacuated with a vacuum pump. An ester with known mass was charged into the cell and then the carbon dioxide was pressured into the cell. The pressure and temperature were adjusted to designated values. After termination of stirring, the phase equilibrium was achieved when the pressure of the system was maintained for 2 h at the given temperature. The samples of the liquid or vapor phases were taken from the lower and the upper valves respectively, and then got into the previously evacuated and weighted small steel vessel through the needle valve and capillary (the volumes were known). During this isothermal process, the pressure inside the autoclave was kept constant by pushing the piston toward the chamber with the screw-driven pump.

**Table 3. Fitted Results for Two Systems CO<sub>2</sub> (1) + EB (2) and CO<sub>2</sub> (1) + PC (2)**

CO <sub>2</sub> (1)+ EB(2) system					CO <sub>2</sub> (1) + PC (2) system				
T/K	$k_{12}$	$c_{12}$	$p_{\text{ARE}}^a/\%$	$y_{\text{ARE}}^b/\%$	T/K	$k_{12}$	$c_{12}$	$p_{\text{ARE}}^a/\%$	$y_{\text{ARE}}^b/\%$
313.0	0.04	-0.03	2.45	0.39	313.0	0.11	0.01	5.44	0.59
333.0	0.08	-0.06	2.90	1.78	333.0	-0.11	0.05	9.57	0.79
353.0	-0.01	0.00	6.16	4.75	353.0	-0.37	0.05	15.96	2.12
373.0	0.02	0.00	5.38	7.28	373.0	0.37	0.08	9.74	1.62

<sup>a</sup> Average relative errors of  $p$ :  $p_{\text{ARE}} = (\sum_{i=1}^n (p_{\text{exp},i} - p_{\text{cal},i}) / p_{\text{exp},i}) / n$ .

<sup>b</sup> Average relative errors of  $y$ :  $y_{\text{ARE}} = (\sum_{i=1}^n (y_{\text{exp},i} - y_{\text{cal},i}) / y_{\text{exp},i}) / n$ .

Therefore, the phase equilibria were maintained through operation. The total mass of the sample was weighted using a balance with an accuracy of 0.0001 g. The volume of the taken sample was determined by measuring the distance between the positions of the piston before and after taking the sample,  $\Delta l$ , and the known inner diameter of the autoclave. The positions of the piston were measured with the help of a Hall probe (model SS541AT) connected to the piston. The uncertainty of  $\Delta l$  was  $\pm 0.1$  mm. The cooled sampling vessel was connected to a glass bulb of known volume. The bulb's temperature was measured with a thermometer. The pressure inside the bulb was measured with an absolute-pressure meter with a precision of 10 Pa. Because the pressure of the desorbed gas was very low (typically about 20 kPa), the mass of CO<sub>2</sub> was easily calculated using the equation of state of an ideal gas. The mass of CO<sub>2</sub> was also calculated using a mass different method (i.e., the mass of vessel before being connected to the glass bulb minus the mass of the vessel after desorbed CO<sub>2</sub>). Therefore, the mole fractions of two phases can be obtained at the given  $p$  and  $T$ . The densities of the vapor and liquid were also obtained by the appropriate mass divided by the volume of each phase. Finally, the molar volumes of mixture were obtained from the densities and the mole fractions of two phases. The above procedures were all repeated for three times. The experimental data listed in Table 1 are the mean values of the measurements. The estimated uncertainty of the mole fractions of the vapor and liquid phases are below 1.7%. The uncertainty in reported densities and mole volumes are estimated to be within 1.9%.

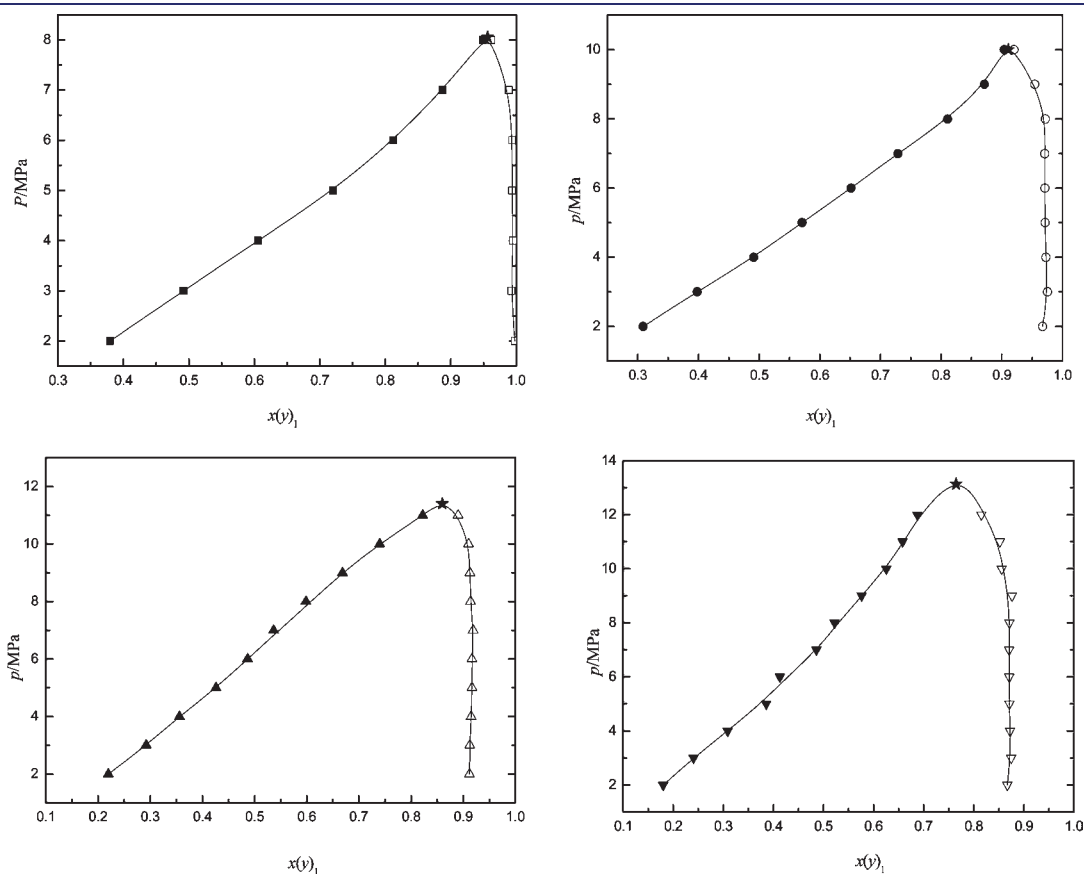


**Figure 2.**  $p-x(y)_1$  diagrams of CO<sub>2</sub> (1) + EB (2) system at four temperatures:  $\blacksquare$ , 313.0 K;  $\bullet$ , 333.0 K;  $\blacktriangle$ , 353.0 K;  $\blacktriangledown$ , 373.0 K;  $\star$ , estimated critical point; —, fitted. Solid points represent the liquid phase, and unfilled symbols represent the gas phase.

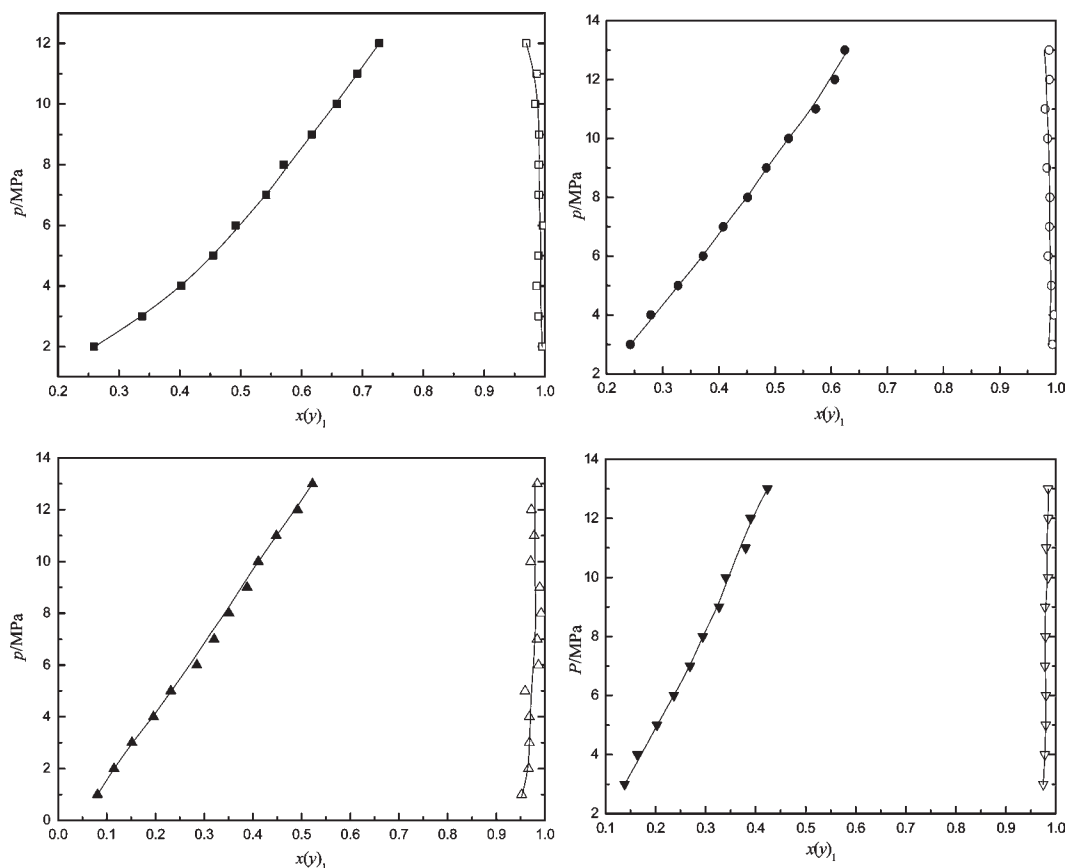


**Figure 3.**  $p-x(y)_1$  diagrams of  $\text{CO}_2(1) + \text{PC}(2)$  system at four temperatures:  $\blacksquare$ ,  $\square$ , 313.0 K;  $\bullet$ ,  $\circ$ , 333.0 K;  $\blacktriangle$ ,  $\triangle$ , 353.0 K;  $\blacktriangledown$ ,  $\triangledown$ , 373.0 K; —, fitted. Solid points represent the liquid phase, and unfilled symbols represent the gas phase.

## CORRELATIONS

The experimental data were correlated with the Peng-Robinson EOS<sup>14</sup> and the conventional mixing rules.<sup>15</sup>

The criterion for phase equilibrium requires that multiple phases at the same  $T$  and  $p$  must be in equilibrium and the fugacity of each component must be the same in all phases. The fitting was performed at each temperature by minimizing the following objective function:

$$F = 5 \sum_{i=1}^N \left( \frac{p - p_{\text{cal}}}{p} \right)^2 + \sum_{i=1}^N \sum_{j=1}^M \left( \frac{y_j - y_{j,\text{cal}}}{y_j} \right)^2 \quad (1)$$

where the subscript cal represents calculated values. Five represents the weighing factor.

When correlating, the critical data ( $p_{c,i}$ ,  $T_{c,i}$ ) and acentric factors ( $\omega$ 's) of the pure components were used which were listed in table 1.<sup>16</sup>

## RESULTS AND DISCUSSION

Isothermal vapor–liquid equilibrium data of  $\text{CO}_2 + \text{ethyl butyrate}$  and  $\text{CO}_2 + \text{propylene carbonate}$  systems were measured at (313.0, 333.0, 353.0, and 373.0) K at pressures between (1.00 and 13.00) MPa. The results are listed in Table 2, where  $x_1$  and  $y_1$  are the mole fractions of  $\text{CO}_2$  in the liquid phase and vapor phase, respectively. The molar volumes of liquid and vapor mixtures at different temperatures ( $T$ ) and pressures ( $p$ ) were obtained from densities and

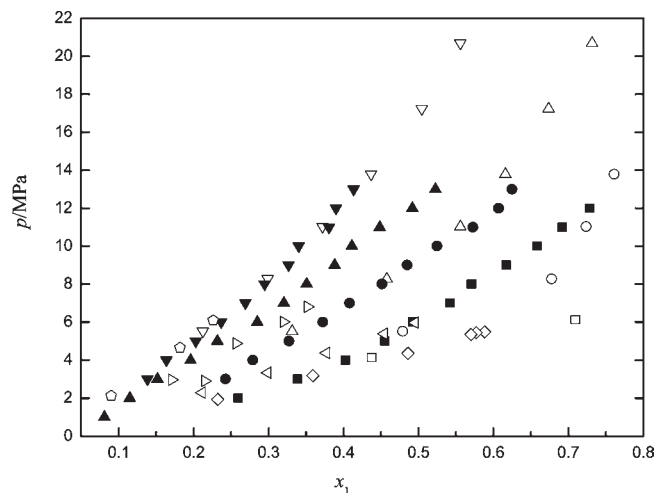


**Figure 4.** Comparison of  $p-x_1$  for  $\text{CO}_2(1) + \text{PC}(2)$  system: this work:  $\blacksquare$ , 313.0 K;  $\bullet$ , 333.0 K;  $\blacktriangle$ , 353.0 K;  $\blacktriangledown$ , 373.0 K. Reference 10:  $\square$ , 298.15 K;  $\circ$ , 308.15 K;  $\triangle$ , 333.15 K;  $\triangledown$ , 373.15 K. Reference 11:  $\diamond$ , 299.85 K; left pointing triangle, 310.95 K; right pointing triangle, 344.25 K;  $\diamond$ , 377.55 K.

mole fractions. The equilibrium ratios ( $K$  factors) are given by

$$K_1 = \frac{y_1}{x_1} \quad \text{and} \quad K_2 = \frac{y_2}{x_2}$$

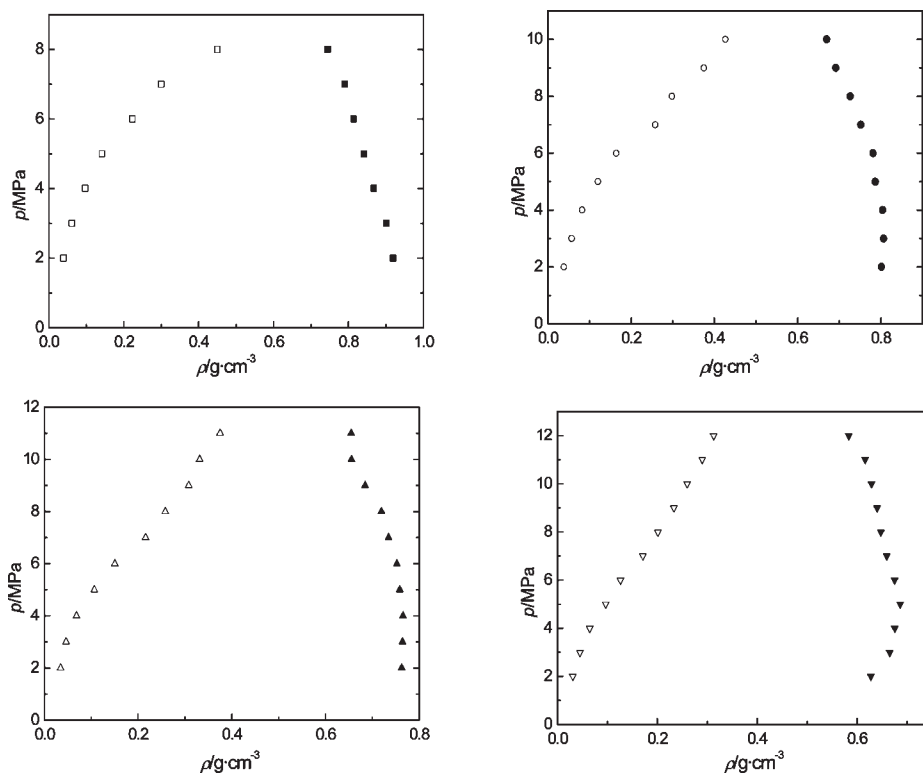


**Figure 5.**  $p$ – $\rho$  diagrams of  $\text{CO}_2$  (1) + EB (2) system at four temperatures:  $\blacksquare$ , 313.0 K;  $\bullet$ , 333.0 K;  $\blacktriangle$ , 353.0 K;  $\blacktriangledown$ , 373.0 K. Solid points represent the liquid phase, and unfilled symbols represent the gas phase.

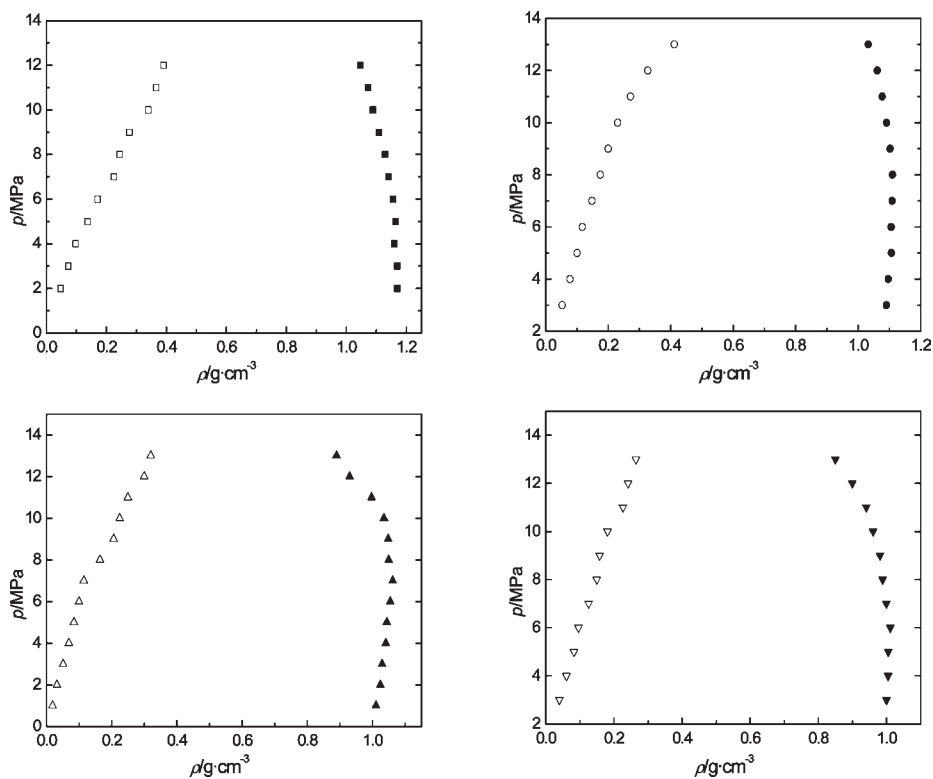


**Figure 6.**  $p$ – $\rho$  diagrams of  $\text{CO}_2$  (1) + PC (2) system at four temperatures:  $\blacksquare$ , 313.0 K;  $\bullet$ , 333.0 K;  $\blacktriangle$ , 353.0 K;  $\blacktriangledown$ , 373.0 K. Solid points represent the liquid phase, and unfilled symbols represent the gas phase.

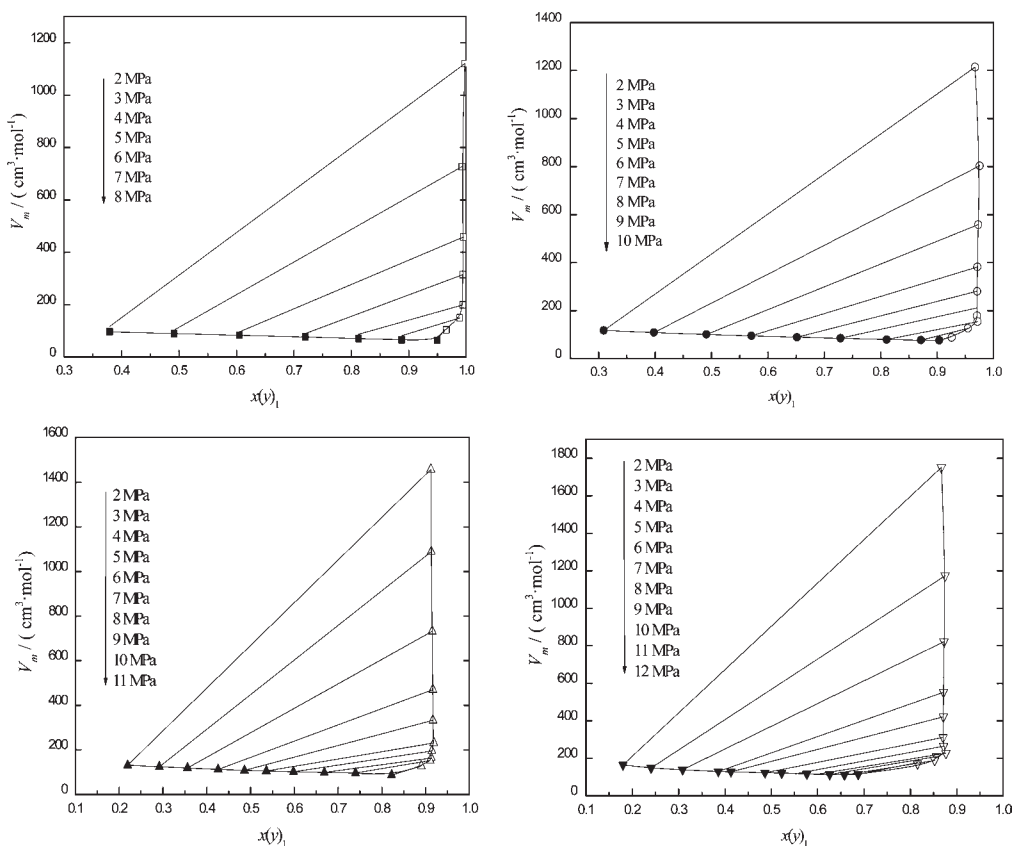


**Figure 7.**  $V_m-x(y)_1$  diagrams of  $\text{CO}_2$  (1) + EB (2) system at different temperatures:  $\blacksquare$ , 313.0 K;  $\bullet$ , 333.0 K;  $\blacktriangle$ , 353.0 K;  $\blacktriangledown$ , 373.0 K; —, isobars. Solid points represent the liquid phase, and unfilled symbols represent the gas phase.

They were also calculated and listed in Table 2. The experimental results were also correlated using the Peng-Robinson EOS with the two-parameter van der Waals mixing rule, and the correlated results were listed in Table 3. From Table 3, it was shown that the binary interaction parameters were different at different temperatures for the two binary systems, but there were not a regular rule. This result was the same as that of Chen.<sup>17</sup>

Figures 2 and 3 give the  $p-x$  diagrams. Figure 4 gives the comparison of this work with the literatures. Figure 5 and Figure 6 give  $p-\rho$  diagrams. Figure 7 and Figure 8 give the molar volumes of vapor and liquid phases, and the thin lines connecting the conjugate points of the two equilibrium phases are isobars and from the upper to lower the pressure are increased.

**Effect of Pressure on the Solubility and Henry's Coefficients of  $\text{CO}_2$  in Liquid Esters.** In Figures 2 and 3, the left-hand lines give the saturation pressures (bubble pressures) as the functions of mole fractions of  $\text{CO}_2$  in liquid phases, the right-hand lines give the saturation pressures (dew pressures) as the functions of mole fractions of  $\text{CO}_2$  in gas phases. It can be observed that the solubilities of supercritical  $\text{CO}_2$  in the two esters are increased with the increasing pressures at the constant temperature, which results in the decrease of densities of the liquid phase. While the solubilities of the two esters in supercritical  $\text{CO}_2$  are also increased with the increasing pressure at a given temperature, thus resulting in increasing the densities of the vapor phase. They can be shown in Figures 5 and 6. Finally, the two lines meet at the critical point at a given temperature. Therefore, only one phase can exist at pressures higher than the critical pressure.

Figure 4 gives the comparison of this work with the literatures for the carbon dioxide + propylene carbonate system. Good agreement was obtained between the data presented here and VLE data published elsewhere at same temperatures.

At the effect of the composition of  $\text{CO}_2$  and the densities together, the molar volumes in the vapor phase is decreasing sharply with increasing pressure at the same temperature. However, there are no remarkable changes in the liquid phase as shown in Figures 7 and 8.

Since the experimental temperatures are higher than the critical temperature of  $\text{CO}_2$  and the pressures are not very high, we can assume reasonably that neglecting all gas-phase nonideality as well as the effect of pressure on the liquid, and also neglecting the interactions between solute and solvent. Using the data in Table 2, the diagrams with the partial pressures of  $\text{CO}_2$  in gas phases against the mole fractions (solubilities) in the liquid were plotted. It was observed that the solubility of SC  $\text{CO}_2$  in the esters is proportional to its partial pressure in the gas phase in a certain range:

$$p_1 = H \times x_1 \quad (2)$$

where  $H$  denotes Henry's coefficient which only depends on the temperature.  $p_1$  is the partial pressure of  $\text{CO}_2$  in the vapor phase. The  $p_{\text{CO}_2} \sim x_1$  lines were presented in Figures 9 and 10. The  $H$ 's values at above four temperatures for the two systems were listed in Table 4 together with the values in literature. At the constant temperature, the  $H$  value is constant, i.e., the relations between

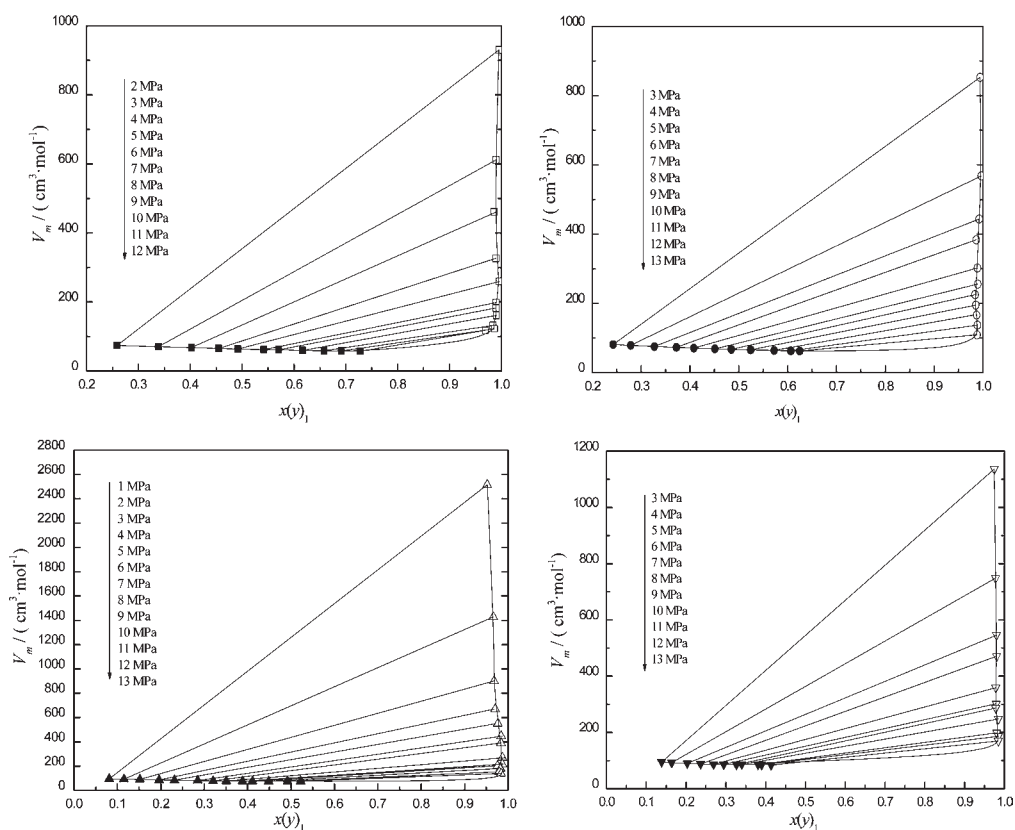


**Figure 8.**  $V_m-x(y)_1$  diagrams of  $\text{CO}_2$  (1) + PC (2) system at different temperatures:  $\blacksquare$ , 313.0 K;  $\bullet$ , 333.0 K;  $\blacktriangle$ , 353.0 K;  $\blacktriangledown$ , 373.0 K; —, isobars. Solid points represent the liquid phase, and unfilled symbols represent the gas phase.

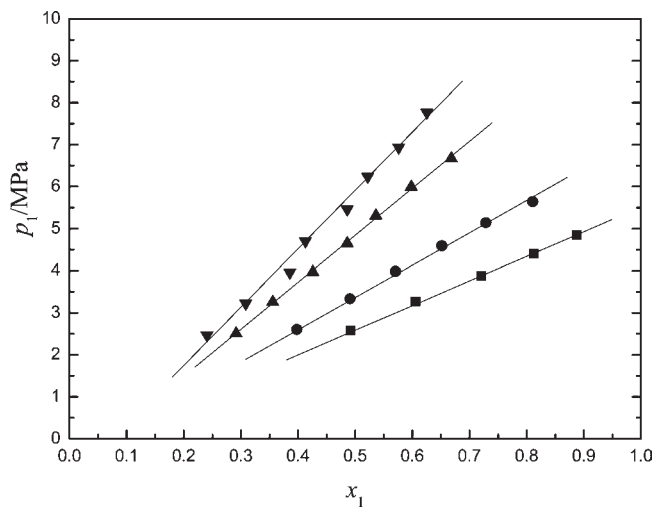


**Figure 9.**  $p_1-x_1$  diagrams of  $\text{CO}_2$  (1) + EB (2) system in the linear range at four temperatures:  $\blacksquare$ , 313.0 K;  $\bullet$ , 333.0 K;  $\blacktriangle$ , 353.0 K;  $\blacktriangledown$ , 373.0 K; —, fitted.

$p_{\text{CO}_2}$  and  $x_1$  are linear, and the fitting correlation coefficients are all greater than 0.995 which can be seen from Table 4. It can be also shown that  $H'$ 's values increased with increasing temperature for the two binary systems, and shown good agreements with literature values. From Figures 9 and 10, it was shown that Henry's law appeared to hold to high pressures and large solubilities for the investigated SC- $\text{CO}_2$  and esters systems.

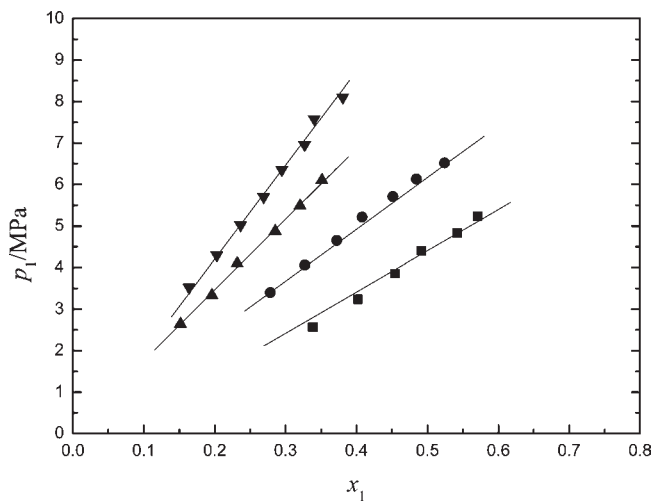


**Figure 10.**  $p_1-x_1$  diagrams of  $\text{CO}_2$  (1) + PC (2) system in the linear range at four temperatures:  $\blacksquare$ , 313.0 K;  $\bullet$ , 333.0 K;  $\blacktriangle$ , 353.0 K;  $\blacktriangledown$ , 373.0 K; —, fitted.

**The Effect of Temperature on the Solubility of SC  $\text{CO}_2$  in the Esters.** Table 2, Figure 2 and Figure 3 show that the solubilities of SC  $\text{CO}_2$  in esters decrease with rising temperature at the constant pressures. The temperature derivative of the solubility, as calculated from the Gibbs–Helmholtz equation, is directly related to either the solution enthalpy or solution entropy of the gaseous solute in liquid mixture. If there are no specific chemical interactions and solvations between solute and



**Table 4. Henry's Coefficients of CO<sub>2</sub> (1) + EB (2) and CO<sub>2</sub> (1) + PC (2) Systems at Various Temperatures**

CO <sub>2</sub> (1) + EB (2)				
T /K	313.0	333.0	353.0	373.0
H/MPa	5.85	7.69	11.17	13.88
R	0.999	0.998	0.995	0.997
CO <sub>2</sub> (1) + PC (2)				
T /K	313.0 (313.15) <sup>a</sup>	333.0 (323.15) <sup>a</sup>	353.0 (343.15) <sup>a</sup>	373.0 (373.15) <sup>a</sup>
H/MPa	9.93 (10.35) <sup>a</sup>	12.46 (12.08) <sup>a</sup>	17.02 (16.60) <sup>a</sup>	22.65 (22.23) <sup>a</sup>
R	0.997	0.995	0.999	0.998

<sup>a</sup>Reference 11.**Table 5. Solution Enthalpy ( $\Delta H_1$ ) and Solution Entropy ( $\Delta S_1$ ) of CO<sub>2</sub> (1) + EB (2) and CO<sub>2</sub> (1) + PC (2) Systems**

CO <sub>2</sub> (1) + EB (2)		
p/MPa	$\Delta_{\text{sol}}H_1/\text{kJ}\cdot\text{mol}^{-1}$	$\Delta_{\text{sol}}S_1/\text{J}\cdot\text{mol}^{-1}$
3.00	-11.90	-34.25
4.00	-11.38	-33.35
6.00	-11.28	-33.06
8.00	-10.17	-29.83
CO <sub>2</sub> (1) + PC (2)		
p/MPa	$\Delta_{\text{sol}}H_1/\text{kJ}\cdot\text{mol}^{-1}$	$\Delta_{\text{sol}}S_1/\text{J}\cdot\text{mol}^{-1}$
6.00	-11.97	-35.06
7.00	-11.40	-33.36
8.00	-10.84	-31.78
9.00	-10.35	-30.31
10.00	-10.78	-31.59

solvent, it makes the activity coefficient of the solute independent of the mole fraction. With those restrictions, it can be shown that

$$\left\{ \frac{\partial \ln x_1}{\partial \left( \frac{1}{T} \right)} \right\} = -\frac{\Delta_{\text{sol}}H_1}{R} \quad (3)$$

and

$$\left\{ \frac{\partial \ln x_1}{\partial \ln T} \right\}_p = \frac{\Delta_{\text{sol}}S_1}{R} \quad (4)$$

where  $x_1$  is the mole fraction of SC CO<sub>2</sub> (solute) at the saturation and  $\Delta_{\text{sol}}H_1$  and  $\Delta_{\text{sol}}S_1$  are the solution enthalpy and the solution entropy of SC CO<sub>2</sub> during dissolution, respectively. By fitting the relation of  $\ln x_1$  with  $1/T$ ,  $\Delta_{\text{sol}}H_1$  and  $\Delta_{\text{sol}}S_1$  were calculated and listed in Table 5. From Table 5, it was shown that there were slight changes for  $\Delta_{\text{sol}}H_1$  and  $\Delta_{\text{sol}}S_1$  at different pressures.

To understand the significance of the solution enthalpy and solution entropy, it is convenient to divide the dissolution process into two parts: condensation and mixing. Thus, the later is common much lower in quantity. Since CO<sub>2</sub> is readily soluble (relatively a large  $x_1$ ) and its temperature coefficient of solubility is negative and large in quantity, the condensation enthalpy of pure solute dominates the dissolution process.

It shows that the different cohesive energy densities are very small.

## CONCLUSIONS

VLE data for the binary systems of carbon dioxide with ethyl butyrate (EB) and propylene carbonate (PC) were measured at (313.0, 333.0, 353.0, and 373.0) K and pressure up to 13.00 MPa. The experimental results were also correlated with the Peng-Robinson EOS with the two-parameter van der Waals mixing rule, and a good agreement was obtained. At the same time, the densities and mole volumes of vapor and liquid phases for the two binary systems are presented. Furthermore, the Henry's coefficients,  $H$ , and solution enthalpy,  $\Delta_{\text{sol}}H_1$ , and solution entropy,  $\Delta_{\text{sol}}S_1$ , of SC CO<sub>2</sub> in the esters at different temperature were also calculated.

## AUTHOR INFORMATION

### Corresponding Author

\*E-mail: zhurongjiao@tju.edu.cn. Tel: +86-22-27406140. Fax: 86-22-27403475.

## REFERENCES

- (1) Fornari, R. E.; Alessi, P.; Kikic, I. High-Pressure Fluid Phase Equilibria: Experimental Methods and Systems Investigated (1978–1987). *Fluid Phase Equilib.* **1990**, *57*, 1–33.
- (2) Dohrn, R.; Brunner, G. High-Pressure Fluid-Phase Equilibria: Experimental Methods and Systems Investigated (1988–1993). *Fluid Phase Equilib.* **1995**, *106*, 213–282.
- (3) Christov, M.; Dohrn, R. High-Pressure Fluid Phase Equilibria Experimental Methods and Systems Investigated (1994–1999). *Fluid Phase Equilib.* **2002**, *202*, 153–218.
- (4) Dohrn, R. High-pressure fluid-phase equilibria: experimental methods and systems investigated (1988–1993). *Fluid Phase Equilib.* **1995**, *106*, 213–282.
- (5) Christov, M.; Dohrn, R. High-pressure fluid phase equilibria: experimental methods and systems investigated (1994–1999). *Fluid Phase Equilib.* **2002**, *202*, 153–218.
- (6) Wong, J.; Johnston, K. Solubilization of Biomolecules in Carbon Dioxide Based Supercritical Fluids. *Biotechnol. Prog.* **1986**, *2*, 29–39.
- (7) Zhu, R.; Zhou, J.; Liu, S.; Ji, J.; Tian, Y. Vapor–liquid equilibrium data for the binary systems in the process of synthesizing diethyl carbonate. *Fluid Phase Equilib.* **2010**, *291*, 1–7.
- (8) Tian, Y.; Zhu, H.; Xue, Y.; Liu, Z.; Yin, L. Vapor-Liquid Equilibria of the Carbon Dioxide + Ethyl Propanoate and Carbon Dioxide + Ethyl Acetate Systems at Pressure from 2.96 to 11.79 MPa and Temperature from 313 to 393 K. *J. Chem. Eng. Data* **2004**, *49*, 1554–1559.
- (9) Cheng, C.; Chen, Y. Vapor–liquid equilibria of carbon dioxide with isopropyl acetate, diethyl carbonate and ethyl butyrate at elevated pressures. *Fluid Phase Equilib.* **2005**, *234*, 77–83.
- (10) Williams, L.; Mas, E.; Rubin, J. Vapor-Liquid equilibrium in the carbon dioxide - propylene carbonate systems at high pressures. *J. Chem. Eng. Data* **2002**, *47*, 282–285.
- (11) Mantor, P. D.; Abib, O.; Song, K. Y.; Kobayashi, R. Solubility of Carbon Dioxide in Propylene Carbonate at Elevated Pressures and Higher than Ambient Temperature. *J. Chem. Eng. Data* **1982**, *27*, 243–245.
- (12) Zubchenko, Y. P.; Shakhova, S. F.; Wei, T.; Titelman, L. I.; Kaplan, L. K. Phase Equilibria and Volume Relationships in the System Propylene Carbonate-Carbon Dioxide. *Zh. Prikl. Khim.* **1971**, *44*, 2044–2047.
- (13) Meder, A.; Tubolkin, A.; Tarat, E.; Durkina, A. Equilibrium in the carbon dioxide + propylene carbonate system. *Zh. Fiz. Khim.* **1974**, *48*, 1985–1987.

- (14) Valderrama, J. The state of the cubic equations of state. *Ind. Eng. Chem. Res.* **2003**, *42*, 1603.
- (15) Soave, G. Equilibrium Constants from a Modified Redlich-Kwong Equation of State. *Chem. Eng. Sci.* **1972**, *27*, 1197–1203.
- (16) Poling, B. E.; Prausnitz, J. M.; O'Connell, J. P. *The properties of gases and liquids*, 5th ed.; McGraw-Hill: New York, 2001.
- (17) Chen, L. High pressure equilibrium and critical curves of binary systems containing supercritical CO<sub>2</sub>. Ph.D. Dissertation; Tianjin University, 2003.